A LUT-based LNA Nonlinear Distortion Compensation Scheme in Direct-Sampling Receivers

Ngoc-Anh Vu[1], Hai-Nam Le[1], Thi-Hong-Tham Tran[2], Van-Phuc Hoang[1], Quang-Kien Trinh[1],
[1]Le Quy Don Technical University, 236 Hoang Quoc Viet Str., Hanoi, Vietnam
[2]Moscow Institute of Physics and Technology, Moscow, Russia
Email: ngocanh220484@gmail.com, namlh@mta.edu.vn

***Abstract*— The paper analyzes the non-linear distortion effects of the Low Noise Amplifier (LNA) in the radio frequency direct-sampling receiver (DRF). A novel look-up table (LUT)-based linearization scheme was proposed. In this scheme, the LNA nonlinearity is estimated by a specialized training-circuit. During the training process, an internally-generated signal with different power levels ranging from the LNA linear region to the saturated region is fed to the training circuit. An LMS algorithm is used to invert the LNA nonlinear coefficients. The estimated coefficients and the corresponding power level of the input signals are stored in a LUT, accessed during the receiving mode, to remove the distortion. The effectiveness of the proposed method is evaluated by a Matlab simulation with four QPSK channels. The simulation results show that the proposed solution significantly enhances the amplification linearity. The Adjacent Channel Power Ratio (ACPR) increases by 40dB, accordingly the spectra of distorted components reduce close to the receiver's background noise level.**

***Keywords*— Direct-sampling RF Receiver, DRF, LNA distortion, digital receiver, LMS algorithm, distortion inversion, multichannel receiver.**

I. INTRODUCTION

THE direct sampling RF receiver (DRF) is a receiver whose signal is fully processed in the digital domain and is known as the ideal Software Defined Radio (SDR). This architecture now has been widely adopted in many commercial devices [1], [2]. By eliminating a number of analog sub-circuits, this structure allows the receiver to work with a wide band, simultaneous multiple-channel reception while maintaining a simple and cost-effective design. Moreover, unlike direct converter receivers (DCR) using analog quadrature mixer [3], [4], this receiver does not encounter inherent problems such as DC offset, IQ imbalance and the nonlinearity of the mixer. In such receiver structure, with the weak signal arriving at the antenna (e.g., close to the background noise level), the amplifying task is vital. So the LNA is an un-replaceable part, especially in the case of a multichannel and wideband receiver. Consequently, the DRF signal might be distorted due to the LNA nonlinearity [5]–[14]. When the total RF signal power from the antenna is higher than the compression point P1dB (Fig. 1), the LNA no longer works in linear region and moves to the nonlinear region, i.e. nonlinear distortions are produced. The distortions consist of harmonics and intermodulation induced from channels with high energy affecting themselves and adjacent channels [8], [12]. The effect of nonlinear LNA depends on the total received RF energy level, therefore its characteristic is mostly unpredictable in the multichannel and wideband receiver. Compensating those distortions in DRF hence is a very challenging task.

To tackle the LNA nonlinearity impacts, many studies have been conducted. Conventionally, the distortion is estimated then is subtracted or inverted from the received signal [6], [13]. The distortion or the components causing distortion are separated by band-pass filters (BPF) as proposed in solutions [6], [13] and [14]. Authors of [12] developed another solution using linear reference receivers to obtain the information. However, these solutions have some practical limitations, for example, using the high-quality BPF filters in the RF domain is difficult [14] and the signal information needed to be filtered must be known in advance [6, 13]. Another approach for power amplifier linearization is LUT method, which was proposed in [11], [15]. This method performs the baseband pre-distortion to linearize the Power amplifier (PA) up to its saturated output power level. The study in [11] presents a solution to linearize PA by adjusting the amplified input signal level to achieve the desired output value. The parameter to adjust the PA input signal level is stored in the LUT table. Thus the cascade of the pre-distorter and the PA looks linear. The proposal in [15] builds a LUT filled with complex gain values of the PA and for each entry of the LUT is one corresponding filter. Both methods in [11], [15] are for the multicarrier transmitter, where the PA takes a relatively strong signal with very-high SNR from the circuitry, and all the general factors about the signal are known, such as amplitude, modulation, shape, duty cycle, and so on. This scenario is basically different from the receiver's side.

In this work, we first carried out a study on the LNA characteristic, which theoretically and experimentally confirmed the fact that the nonlinearity of LNA mainly depends on the total power level of the input signals. This is consistent with the results in [6]-[13]. From this analysis, a novel LUT-based method to compensate the LNA nonlinearity in multichannel DRF is proposed.

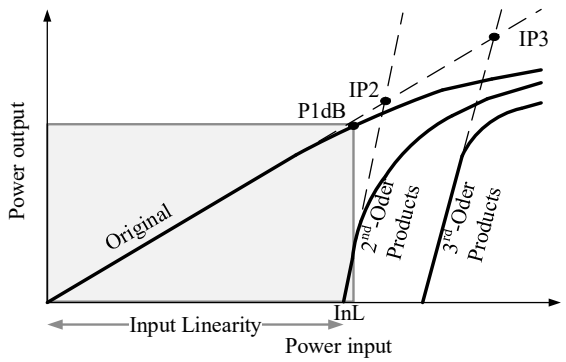

Fig. 1. LNA Input-Output power characteristics

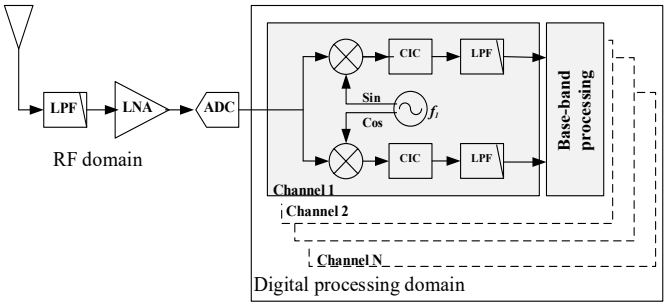

Fig. 2. The architecture of multichannel DRF.

We use a built-in digital training circuit to pre-evaluate the nonlinear characteristic of the LNA with respect to the input signal power level. These parameters are then stored in a LUT for the process of recovering the received signal during the working mode. With this structure, only one distortion compensation circuit is required for all carrier frequency channels and the distortion is mitigated right at the RF domain. The training process is performed separately with the receiving process so this method does not involve LMS circuit in the distortion removal step as in [7]–[9], [12], hence reduces the power consumption and other timing issues. The proposed scheme does not use the reference receiver, so compared to the approach in [7]–[9], [12], it is more advanced in the hardware cost, energy consumption, and design complexity.

The following of the paper is organized as follows. Part II presents the effect of nonlinear distortion of LNA in DRF and the equivalent nonlinear model. Part III presents a solution to reduce distortion based on training in finding nonlinear inverse parameters of LNA according to different levels of LNA output signal. The simulation test results and conclusions are drawn in section V.

II. LNA NONLINEARITY MODEL

A. LNA nonlinear distortion model

In DRF (Fig.2), the main role of LNA is to amplify linearly the weak signals at the receiver's antenna, which are close to the background noise [7]–[11]. This can be achieved in a very

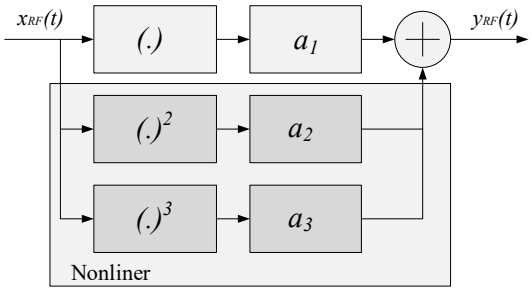

Fig. 3. A simplified non-linear model of LNA in DRF.

limited input energy range, i.e. when the total input power level is lower than P1dB value. While considering the distortion orders in narrowband multi-channel receivers, it is sufficient to notice only intermodulation products appearing close to distorted channels [13], [12]. However, with wideband DRF, the impact of all harmonic and intermodulation components needs to be taken into consideration [17]. As a matter of fact, in such wideband multichannel DRF, when LNA works nonlinearly, the generated components are the combinations of all RF channels into the receiver, so the resulting distortion is inherently complex. The non-linear distortion model for RF signals is assumed to be a the form of a basic polynomial [3,16] .

$$y_{RF}(t) = \sum_{i=1}^{k} a_i(t) x_{RF}^i(t) \quad (1),$$

where $x_{RF}(t)$ and $y_{RF}(t)$ are LNA inputs and outputs, respectively; $a_i(t)$ is the i-th nonlinear coefficient. The input signal $x_{RF}(t)$ can be written as

$$x_{RF}(t) = 2Re[x(t)e^{j\omega_c t}] = x(t)e^{j\omega_c t} + x^* e^{-j\omega_c t} \quad (2),$$

Where $x(t)$ is the baseband signal of $x_{RF}(t)$, $x(t)$ can be a signal with one carrier frequency or multiple carrier frequencies; $\omega_c = 2\pi f_c$, where f_c is the central carrier frequency and (.) * represent the complex conjugate.

The bandwidth of DRF is often large (several tens to hundreds of MHz). Therefore, the signal of a channel can be affected by harmonic and intermodulation components generated from far away channels, and the nonlinear model in (1) can be applied. However, in practice, it is sufficient to consider up to the third-order components because the higher ones are relatively small and can be ignored [7]–[9]. With that assumption, the simplified model is depicted in Fig. 3, and is expressed as follows

$$y_{RF}(t) = a_1 x_{RF}(t) + a_2 x_{RF}^2(t) + a_3 x_{RF}^3(t) \quad (3)$$

The second-order and third-order are fully derived as follows

$$x_{RF}^2(t) = 2A^2(t) + x^2(t)e^{2\omega_c t} + [x^*(t)]^2 e^{-j2\omega_c t} \quad (4),$$

$$a_3 x_{RF}^3(t) = a_3\{x(t)e^{j\omega_c t} + x^*(t)e^{-j\omega_c t}\}^3$$
$$= a_3\{x^3(t)e^{j3\omega_c t} + 3x^2(t)x^*(t)e^{j\omega_c t} + 3x(t)[x^*(t)]^2 e^{-j\omega_c t} + [x^*(t)]^3 e^{-j3\omega_c t}\} \quad (5)$$

Where $2x(t)x^*(t) = 2A^2(t)$ is the component that appears around the baseband.

In (4), generated distortions occur both at DC and $\pm 2\omega_c$ but not at ω_c. This ensures that the second-order distortion does not affect itself and the neighboring channels, but affects the channels surrounding $2\omega_c$.

If the carrier frequency is high, then the second-order component in (4) is outside the operating range of the receiver and only the third-order component is considered. From (5) the third-order components generate distortions around ω_c ($3x^2(t)x^*(t)e^{j\omega_c t}$ component) affecting itself and adjacent channels, and the component $x^3(t)e^{j3\omega_c t}$ affecting channels around $3\omega_c$. This infers that with any carrier frequency, the third order component imposes direct distortion around the interested bandwidth (i.e., around ω_c).

B. *Experimental measurement of LNA nonlinear distortion and characteristics*

The current LNA with a small noise figure, good gain factor, and adequate IP-x positions (see Fig. 1) is suitable for wideband receivers. Also, it experiences very little variation within the receiver's frequency range. Indeed, from the provided experimental results, two commercial Mini-Circuit LNA ZX60-P105LN+ [18] and ZFL-500LN+ [19], the amplification coefficient ZFL-500LN+ varies less than 0.7dB with the frequency range from DC to 500MHz; the amplification coefficient of ZX60-P105LN+ varies less than 1dB in the frequency range from close to DC to 2.6GHz.

We examined in more detail the ZFL-500LN+ parameter with frequency signals at 5.3MHz, 50MHz and 125MHz. The results show that the parameters include amplification, the nonlinearity of 2nd-order and 3rd-order at all 3 frequencies almost the same (Fig. 4). The survey results of ZFL-500LN+ also show that the nonlinear parameters of LNA are also uniform throughout the working range.

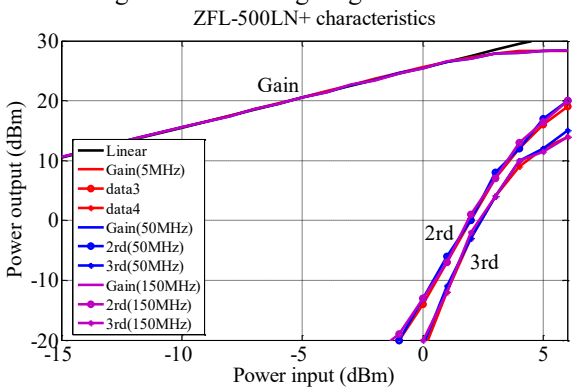

Fig. 4. ZFL-500LN+ parameters with different input frequency (5.3MHz, 50MHz, and 125MHz)

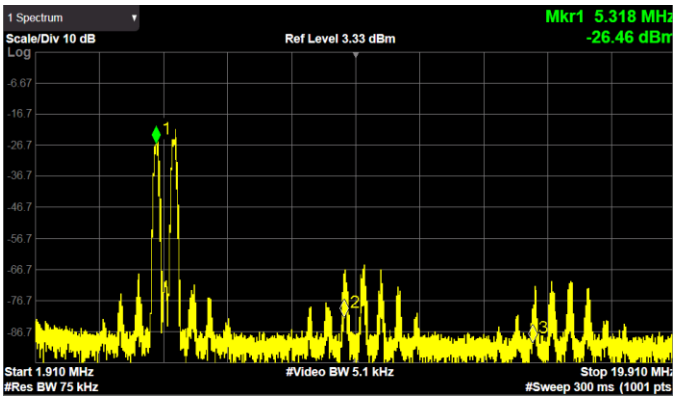

Fig. 5. ZFL-500LN+ RF output signal spectrum with 2 QPSK channels

For the multichannel test case, two channels of QPSK signals at frequencies of 5.3MHz and 5.8MHz are generated with the power of -4dBm. The signal spectrum after LNA is shown in Fig. 5. From the figure, harmonics and intermodulation appear around these two channels and some remote locations, which is consistent with the models in (3)–(5). The resulting distortion also affects the receiver channels at the same frequency position.

III. LINEARIZATION METHODS

A. *Structure of the DRF receiver with proposed nonlinear distortion compensation*

The structure of DRF with the proposed LNA nonlinear distortion compensation scheme is shown in Fig. 6. There are two working modes: training and receiving, selected by a dedicated RF multiplexer. In both modes, the main receiver directly samples the signal of the entire frequency range using a high-speed ADC. Multiple channels with different modulation types and carrier frequencies can be received simultaneously. For the training mode, a signal generator is added into the receiver structure to create the training input for constructing LNA characteristics. After completing the training process, the multiplexer switches to receiving mode.

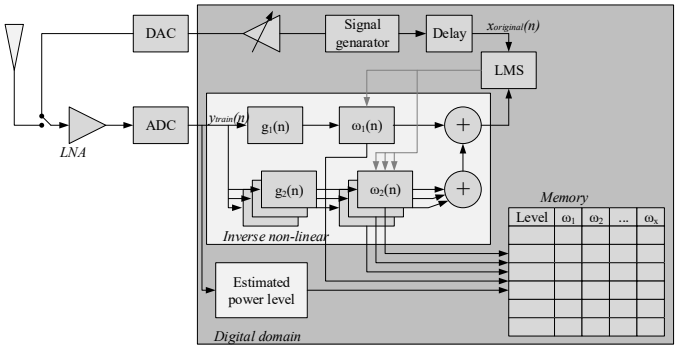

Fig. 6. Reduced diagram of the DRF in the training mode

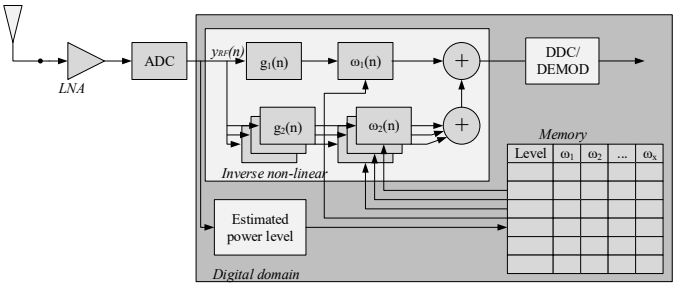

Fig. 7. Reduced diagram of the DRF in the receiving mode

In the training mode, the reference RF signal is internally-generated and converted into an analog signal by a digital-to-analog converter (DAC). This signal is fed to the main receiver via an input multiplexer.

A 2-tone reference RF signal (consisting of 2 different frequency sine waves) is used for the training. The power level of the training input is varied in the interested range of the LNA input power with an adequate resolution. The LMS circuit adjusts the coefficient to fit the output of the inverse non-linear model with the original 2-tone signal. As a result, the final converged nonlinear coefficients of the model characterize the inverse model in (3). The parameters corresponding to each input power level are obtained and stored in a memory (i.e., LUT) for further use in the receiving mode.

In the receiving mode, after being digitized by the ADC, the multiple carrier frequency channels with different types of signal modulation are fed to a power estimation block and the compensation circuit, i.e., the inverse nonlinear model. As the signal feeding is performed in the digital domain, 2 paths can intake the same signal level, which has been an issue for the approach of the reference receiver in the analog domain [7]–[9], [12]. The inverse scheme used in training is employed again now in the distortion removal process. According to the input level determined by the envelope detector circuit, the nonlinear coefficients of the model are updated and retrieved from the LUT. This task repeats continuously to ensure that the distortion is always corrected throughout the receiving process. As a result, the model compensates all the distortions caused by LNA non-linear impact without affecting other operations of the receiver.

B. The Training Algorithm

As mentioned before, we use a conventional 2-tone reference RF signal consisting of two different frequency sine waves to extract the inverse distortion characteristics [17]. The input power levels are determined as shown in Fig. 8. For each level, a set of LNA inverse parameters is determined by the LMS circuit. The diagram of the implementation of training and inverting the distortion is shown in Fig. 6.

The sampled distorted signal from the main path $y_{train}[n]$ is fed directly to the nonlinear compensation circuit while the sampled generated signal $x_{train}(n)$ is passed to the LMS circuit to adjust the coefficients $w_i(n)$. This circuit will adjust the inverse model to fit the function (6).

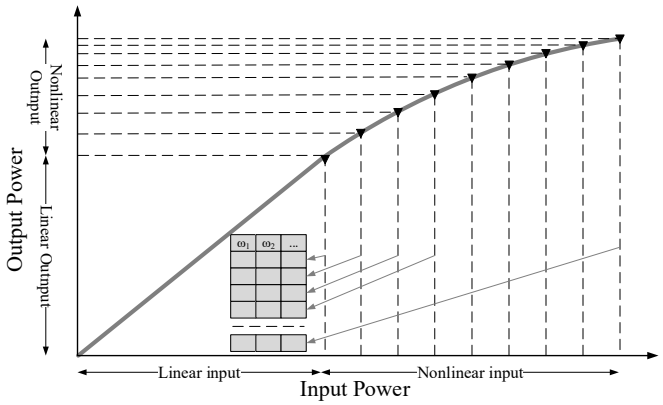

Fig. 8. Equally-dividing LNA input signal level and output signal level

$$\hat{x}_{train}(n) = F_{INV}(y_{train}(n)) = F_{INV}(x_{train}(n) + e(n)) \quad (6)$$

Where F_{INV} represents the mathematical model of the inverse model circuit. As $\hat{x}_{train}$ is approaching the original $x_{train}(n)$, the F_{INV} fits the inverse function of the LNA,F_{LNA}^{-1}. As a result, the final output $\hat{x}_{train}[n]$ is expected to have only the linear components as the non-distorted $x_{train}(n)$. The distorted component e(n) is removed by the inverse nonlinear model.

Let's denote $g_i(x[n])$ is the i-th order of the main receiver input $y_{training}[n]$, thus

$$g_i(y_{train}[n]) = y_{train}^i[n], \text{ i = 1,2,…k} \quad (7)$$

The current output of the compensation circuit expressed as

$$\hat{x}_{train}[n] = \sum_{i=1}^{k} \hat{w}_i[n] g_i(y_{train}[n]) \quad (8)$$

This output is fed back to the LMS block, where it is subtracted from the reference input $y_{REF}(n)$ for calculating the error

$$\hat{\varepsilon}[n] = x_{train}(n) - \sum_{i=1}^{k} \hat{w}_i[n] g_i(y_{train}[n]) \quad (9)$$

The LMS principally operates to minimize the square error $\hat{\varepsilon}[n]^2$ in (9). The nonlinear coefficient $\hat{w}_i[n]$ adjusts as follows

$$\hat{w}_i[n] = \hat{w}_i[n-1] + \mu_i f_i(y_{train}[n])\hat{\varepsilon}[n] \quad (10)$$

This process continues until all coefficients $\hat{w}_i[n]$ stabilize at a fixed value or varies under the desired threshold, at that time the square error reaches the minimum. During the approximation process, $\hat{x}_{train}[n]$ is asymptotically approaching the linear reference input $x_{train}(n)$ After the LMS converged, the output signal $\hat{x}_{train}[n] \approx x_{train}(n)$. Thus, the transfer function of the compensation circuit at the LMS convergence is the inverse of the LNA's transfer function. The set of converged parameters and the corresponding input power level are stored in the memory.

These parameter sets will be used for recovering the original signal from the distorted one during the reception process, this will be detailed in Section III.4.

IV. EVALUATION OF THE PROPOSED COMPENSATION TECHNIQUES

A. Training mode for DRF receiver

The inverse coefficients of the nonlinear model were calculated as presented in III.B. The LNA parameters used in the simulation including gain factor, 2nd order nonlinear parameter, 3rd order nonlinear parameter, have been rigorously calibrated from measurement data on ZFL-500LN+ [19]. In the simulation, a two-tone reference signal of 5.3MHz and 5.8MHz is fed to the DAC and the receiver's LNA input. With the input signal level changing from -14dBm to +6dBm, the LNA output at certain points will be distorted. The input power range of the two-tone signal from -14 ÷ 6dBm is divided into 2^N intervals.

The AM-AM characteristics of the training curve are shown in Fig. 9. In this figure, the solid-black and the red dashed line represent the direct and inverse LNA characteristic, respectively. The average of those characteristics is the compensated characteristic, which fairly fits the ideal linear characteristic.

The parameters received after training are stored in a LUT memory and will be used for compensating LNA nonlinearity in the receiving mode.

B. Evaluating DRF performance in Receiving Mode

To evaluate the effectiveness and study the Adjacent Channel Power Ratio (ACPR) concerning the LUT resolution, we further set up a test case for a wideband multichannel DRF. In this test, four QPSK modulation channels with parameters of the channels are given in TABLE I . The three channels with RF signal input power level is set to be ~30dBm. Channels Ch2, Ch3 and Ch4 are chosen to be close to each other (with the spacing about 100kHz), they hence can distort each other by the odd-modulated intermodulation components. Channel Ch4 with the smallest signal power level (-75 dBm) is the most seriously affected by the 3rd intermodulation from Ch2 and Ch3. At the same time, channel Ch4 with 5.395 MHz carrier frequency will also be affected by the 2nd harmonic of channel Ch1.

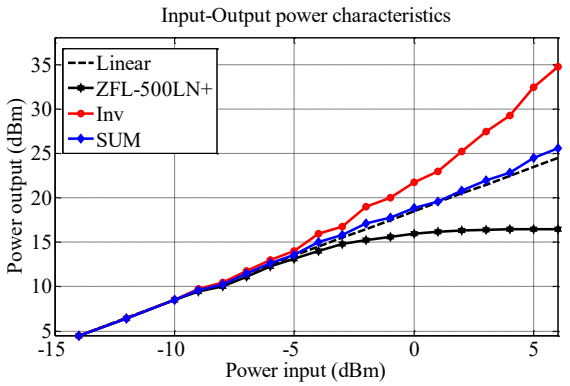

Fig. 9. AM-AM characteristics of LNA before and after distortion correction

TABLE I . CONFIGURATION OF 4 SIMULATED QPSK CHANNELS IN THE IMPLEMENTED RX.

	Type	Symbol rate/Power	RF Carry Frequencies
Ch1	QPSK	24 kbps, -30 dBm	$f_1 = 2.700$ MHz
Ch2	QPSK	24 kbps, -30 dBm	$f_2 = 5.200$ MHz
Ch3	QPSK	24 kbps, -30 dBm	$f_3 = 5.300$ MHz
Ch4	QPSK	24 kbps, -75 dBm	$f_4 = 5.395$ MHz

TABLE II . ACPR AT THE OUTPUT OF THE COMPENSATION CIRCUIT OF CHANNEL CH4.

Size LUT	8	16	32	64	128
ACPR	~15 dB	~21dB	~27 dB	~33 dB	~40 dB

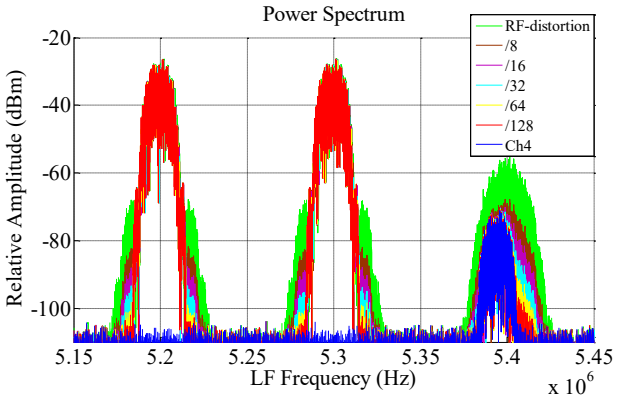

Fig. 10. Analysis of the DRF performance with respect to the LUT size, spectra of the RF signals before and after compensation

To check the impact of the LUT resolution on DRF performance, we have simulated LUT with different number of data points, from 8 to 128. The spectra of the output signals of DRF with and without the compensation are plotted in Fig. 10.

From the spectra, it can be seen that, the most affected channel is Ch4, which is distorted by the 2nd harmonic of Ch1 and the 3rd order distortion of Ch2 and Ch3, as mentioned above.

The ACPR of Ch4 is measured to confirm the compensation effect with corresponding resolutions of the LUT size. ACPR of channel Ch4 at the output of the compensation circuit is presented in TABLE II. The result in TABLE II shows that the higher the resolution of the training process, the better the distortion mitigation effect. When the size is 128, the distortion component at channel Ch4 mostly reduces close to the background noise and the ACPR increases by 40 dB.

V. CONCLUSIONS

In this paper, based on the analysis of the LNA properties, which are relatively uniform in terms of parameters by frequency and impact in DRF, a new LUT-based distortion compensation scheme was proposed. The scheme characterizes the distortion parameters by the training circuit with the LMS algorithm. The parameters are then stored in the LUT for further use. In the actual receiving process, depending on the total received signal power level, the scheme access this LUT and update the coefficients to mitigate the corresponding nonlinearity. Due to the separated training and receiving modes, there is practically no LMS circuit in mitigation process, hence the timing issue might be relaxed.

A DRF with 4QPSK channels is set up to test the proposed method's effectiveness. The simulations with different LUT resolution are implemented. The results show that the spectrum of the distortion component is reduced significantly. The ACPRs of the distorted channels are also improved and depend on the LUT resolution. The proposed method has totally digital structure and simple operation modes, features that are well-suited for application in nowadays telecommunication systems.

ACKNOWLEDGEMENT

This research is funded by the Vietnam National Scientific Research under grant Project number ĐTĐLCN.33/17.

REFERENCES

[1] Software Defined Radio, Spectrum Analyzer, and Panoramic Adapter/ Available: http://www.rfspace.com/RFSPACE/SDR-IQ.html. [Accessed May 20, 2019].

[2] Perseus SDR - Software Defined 10 kHz - 30 MHz Receiver. Available: http://microtelecom.it/perseus/. [Accessed May 20, 2019].

[3] O. Jamin, *Broadband Direct RF Digitization Receivers*, Analog Circuits and Signal Processing 121, DOI 10.1007/978-3-319-01150-9_2, Springer International Publishing Switzerland 2014

[4] L. Anttila, M. Valkama, and M. Renfors, "Circularity-based I/Q imbalance compensation in wideband direct-conversion receivers," *IEEE Trans. Veh. Technol.*, vol. 57, no. 4, pp. 2099–2113, Jul. 2008.

[5] A. A. Abidi, "Direct-conversion radio transceivers for digital communications," *IEEE J. Solid-State Circuits*, vol. 30, no. 12, pp. 1399–1410, Dec. 1995.

[6] R. Vansebrouck, O. Jamin, P. Desgreys, and V.-T. Nguyen, "Digital distortion compensation for wideband direct digitization RF receiver," *in Proc. IEEE 13th Int. New Circuits Syst. Conf. (NEWCAS),* Jun. 2015, pp. 1–4.

[7] Ngoc-Anh Vu, Hai-Nam Le, Thi-Hong-Tham Tran and Quang Kien Trinh, "Novel Distortion Compensation Scheme for Narrowband Multi-channel Direct RF Digitization Receiver," *2019 19th International Symposium on Communications and Information Technologies (ISCIT'19)*, Sep 2019

[8] Ngoc-Anh Vu, Thi-Hong-Tham Tran, Quang Kien Trinh and Hai-Nam Le, "LNA Nonlinear Distortion Impacts In Multichannel Direct RF Digitization Receivers And Linearization Techniques," *Research in Intelligent and Computing in Engineering 2019*, Aug 2019

[9] Ngoc-Anh Vu, Hai-Nam Le, Thi-Hong-Tham Tran, Quang Kien Trinh and Van-Phuc Hoang, "Adaptive Distortion Inversion Technique for LNA's Nonlinearity Compensation in Direct RF Digitization Receivers", *2019 International Conference on Advanced Technologies for Communications (ATC)*, Oct 2019

[10] Andersson, S. (2006). *Multiband LNA design and RF-sampling front-ends for flexible wireless receivers.* Phd thesis, Linko¨ping University.

[11] K. J. Muhonen, M. Kavehrad and R. Krishnamoorthy, "Look-up table techniques for adaptive digital predistortion: a development and comparison," *in IEEE Transactions on Vehicular Technology*, vol. 49, no. 5, pp. 1995-2002, Sept. 2000.

[12] Jaakko Marttila, Markus Allénand Marko Kosunen, "Reference Receiver Enhanced Digital Linearization of Wideband Direct-Conversion Receivers" *IEEE Transactions On Microwave Theory And Techniques*, vol.65, no. 2, pp. 607-620, February 2017.

[13] M. Grimm, M. Allen, J. Marttila, M. Valkama, and R. Thoma, "Joint mitigation of nonlinear rf and baseband distortions in wideband direct-conversion receivers," Microwave Theory and Techniques, IEEE Transactions on, vol. 62, no. 1, pp. 166–182, Jan 2014.

[14] Raphaël Vansebrouck, Chadi Jabbour, Olivier Jamin, and Patricia Desgreys, "Fully-Digital Blind Compensation of Non-Linear Distortions in Wideband Receivers" *IEEE Transactions on circuits And Systems-I: Regular Papers*, vol. 64, no. 8, pp. 2112-2123, August 2017.

[15] P. Jardin and G. Baudoin, "Filter Lookup Table Method for Power Amplifier Linearization," *in IEEE Transactions on Vehicular Technology*, vol. 56, no. 3, pp. 1076-1087, May 2007.

[16] M. Valkama, A. Shahed Hagh Ghadam, L. Anttila, and M. Renfors, "Advanced digital signal processing techniques for compensation of nonlinear distortion in wideband multicarrier radio receivers," *IEEE Trans. Microw. Theory Techn.*, vol. 54, no. 6, pp. 2356–2366, Jun. 2006.

[17] Admoon Andrawes "Multi-tone Analysis in Nonlinear Systems," 2nd International Conference on Advances in Computational Tools for Engineering Applications (ACTE), pp. 96-100, 2012.

[18] ZX60-P105LN+ http://www.minicircuits.com

[19] ZFL-500LN+ http://www.minicircuits.com